Earth Reinforcement Practice, Ochiai, Hayashi & Otani (eds) © 1992 Balkema, Rotterdam. ISBN 90 5410 093 1

Prediction of the deformation of reinforced embankments by centrifuge experiments

H.Abe, Y.Kitamoto, M.Honda & R.Jinki
Kajima Technical Research Institute, Kajima Corporation, Tokyo, Japan

ABSTRACT: When extensible materials, such as geogrids, are used in reinforced embankments, the reinforcement effect comes into operation with the progress of the deformation in the embankment. In evaluating the actual stability of such embankments, therefore, the deformation of the embankments needs to be taken into account. In this study, centrifuge model tests were carried out on reinforced embankments and the test results were compared with the calculation results which took account of the deformation. As a result, it was observed that the slip surface becomes planar with steep slopes, and that the failure height and crest settlement of the embankments could be evaluated by calculation.

1 INTRODUCTION

In land development and road construction in recent years, there has been an increasing number of cases where steep embankments are constructed with the aim of ensuring effective use of the available land by using reinforcement materials to increase the shear resistance. When relatively extensible reinforcement materials, such as geogrids, are used, their reinforcement effect comes into operation with the progress of the deformation of the embankments. In the limit equilibrium methods, which are generally applied to stability analysis of reinforced embankments for engineering practice, however, the displacement of the slip soil is usually not taken into account, resulting in inaccurate assessment of the reinforcement effect.

The authors, being of the opinion that the deformation occurring in the embankments should be taken into account in evaluating the stability of reinforced embankments, devised an equation showing the relationship between the shear displacement and shear stress due to the tensile force accompanying shear in the reinforcements traversing the slip surface (Abe & Kitamoto, 1990). If this equation is applied to the stability analysis of reinforced embankments, it becomes possible to evaluate the stability from both the reinforcement effect (the so-called "safety factor") and the deformation of the embankment. In order to examine the practical applicability of this evaluation method, tests were conducted on centrifuge models on which the stress conditions that occur at the level of actual structures could be reproduced.

2 CONCEPT OF REINFORCEMENT EFFECT

2.1 Pull-out resistance of embedded reinforcement

The pull-out resistance of the reinforcements in the soil must first be evaluated in discussing the stability of a reinforced embankment. In the case of a reinforcement that gives a linear relationship between the tensile force and strain under tensile loading in air, because the strain distribution in the reinforcement under pull-out loading exhibits an approximately triangular shape that gives the maximum value at the pull-out end, the relationship between the pull-out resistance P_r and the elongation Δl can be represented by the following equation (Abe & Kitamoto, 1989).

$$P_r(\Delta l) = \frac{T}{\sqrt{L_{rl}\varepsilon_l}}\sqrt{2\Delta l} \qquad (1)$$

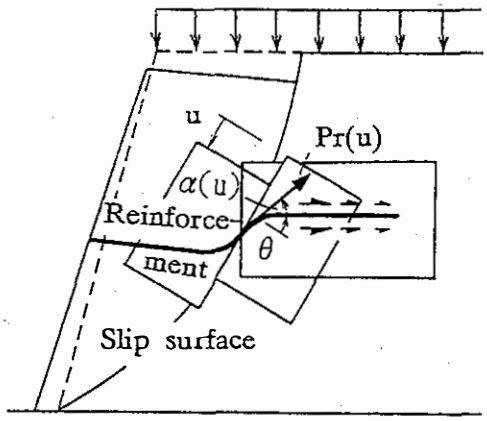

Figure 1 Concept of reinforcement effect

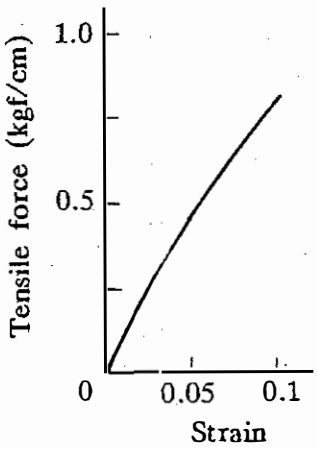

Figure 2 Tensile characteristics

where,

T, ε : tensile strength of reinforcement with width W_r and corresponding strain

L_{rl} : minimum anchorage length required for occurrence of failure, given by the following equation,

$$L_{rl} = \frac{T}{2 W_r \sigma_n f_b \tan\phi} \tag{2}$$

where,

σ_n : normal stress acting on reinforcement

ϕ : internal friction angle of soil

f_b : coefficient of reinforcement bond (Jewell et al., 1985)

If the anchorage length L_r is greater than L_{rl}, P_r will increase with Δl in accordance with Equation (1) and failure will occur when $P_r = T$. If, on the other hand, L_r is smaller than L_{rl}, pull-out will occur when P_r has reached the state represented by Equation (3) and P_r will maintain the same value thereafter.

$$P_r = 2 L_r W_r \sigma_n f_b \tan\phi \tag{3}$$

2.2 *Increase in shearing resistance due to reinforcement*

Given the deformation pattern shown in Figure 1, an increase in the shear displacement will result in tensile force being generated in the reinforcement traversing the slip surface. If the tensile force is equivalent to the pull-out resistance of the reinforcement, the relationship between the shear resistance R_{ext} that increases with the tensile force under direct shear conditions and the shear displacement u can be expressed by Equation (4), and this together with what was said in Section 2.1 elucidates such phenomena as the pull-out and failure in the anchorage of the reinforcement due to the interaction with the surrounding soil (Abe & Kitamoto, 1990).

$$R_{ext}(u) = P_r(\Delta l)\sin\{\theta+\alpha(u)\} + P_r(\Delta l)\cos\{\theta+\alpha(u)\}\tan\phi \tag{4}$$

where,

θ : initial angle of reinforcement from normal of slip surface

$\alpha(u)$: bending angle increasing with shear, given by the following equation,

$$\sin^2\alpha(u) = \frac{\cos^2\theta}{\cos^2\theta + \left(\frac{L_0}{u} + \sin\theta\right)^2} \tag{5}$$

where,

L_0 : length of reinforcement participating in bend

The elongation of the reinforcement due to u needs to be calculated for Δl in Equation (4). Because the deformation of the reinforcement accompanying shear is circular, this may be calculated as follows from geometrical conditions.

$$\Delta l(u) = \frac{L_0}{2}\left\{\frac{\alpha(u)\cos\theta}{\cos\{\theta+\alpha(u)\}\tan(\alpha(u)/2)} - 1 - \frac{\cos\theta}{\cos\{\theta+\alpha(u)\}}\right\} \tag{6}$$

That is, the tensile force P_r in Equation (4) can be obtained by substituting Equation (6) for Δl in Equation (1). From the foregoing, the stability evaluation of a reinforced embankment taking account of the deformation due to shear

displacement is made possible if R_{ext} is taken into account for all reinforcements crossing the slip surface.

3 TEST CONDITIONS AND PROCEDURE

The stability evaluation test described below was carried out assuming a reinforced embankment on hard ground.

3.1 Testing materials

The properties of the embankment and reinforcement materials are shown in Table 1. The embankment materials were air-dried sand with a uniformity coefficient of U_c = 2.1, and an internal friction angle of ϕ = 37.4° at a relative density of D_r = 60%.

In selecting the reinforcement materials, care needs to be taken over the tensile strength T, failure strain ε_1 and the coefficient of reinforcement bond f_b, which are the main factors influencing the reinforcement effect (Kitamoto & Abe, 1991). Here, reinforcement materials that had the tensile force-strain relationship shown in Figure 2 were used and sand particles were bonded to the whole of the surface of the reinforcements so that $f_b = 1$ (i.e. the bond condition between the sand and the reinforcement would be the same as the friction condition of the sand itself).

3.2 Centrifuge model test

A 5cm-thick wooden board was placed in the testing box (width: 70cm, height: 30cm, depth: 15cm) and a reinforced embankment of 15cm in height and with 6 reinforcement layers, in which the slope sections were wrapped at vertical intervals of 2.5cm, was created on the wooden board (see Figure 3). The sand was compacted to a density of 1.6×10^3kg/m^3 (equivalent to D_r = 60%) and displacement gauges were installed at 3 points to measure the crest settlement. The tests were carried out for the 6 cases given in Table 2. The aim in Cases 1 to 4 was to examine the influence of the reinforcement length and slope gradient on the failure mode and the embankment height at the time of the collapse. In Cases 5 and 6, an attempt was made at evaluating the stability of the embankment that varies with the deforma-

Table 1 Characteristics of materials used

Embankment materials		
Specific gravity	Gs	2.69
Uniformity coefficient	Uc	2.1
Cohesion	c	0kgf/cm^2
Internal friction angle	ϕ	37.4°
Reinforcement materials		
Tensile strength	T	0.8kgf/cm
Failure strain	ε_1	0.1
Coefficient of reinforcement bond	f_b	1

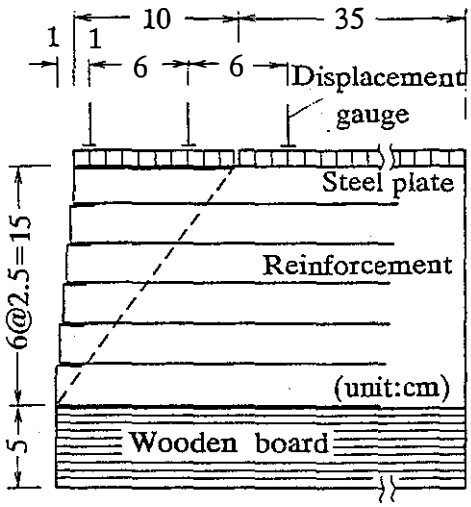

Figure 3 Model embankment (Case 5)

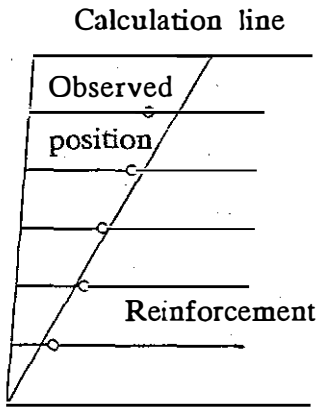

Figure 4 Slip line (Case2)

Table 2 Test cases

Case	Slope gradient	Reinforcement length	Load on embankment
1	1:0.07	5cm	No
2	1:0.07	10cm	No
3	1:0.07	20cm	No
4	1:0.5	10cm	No
5	1:0.07	20cm	Yes
6	1:0.5	20cm	Yes

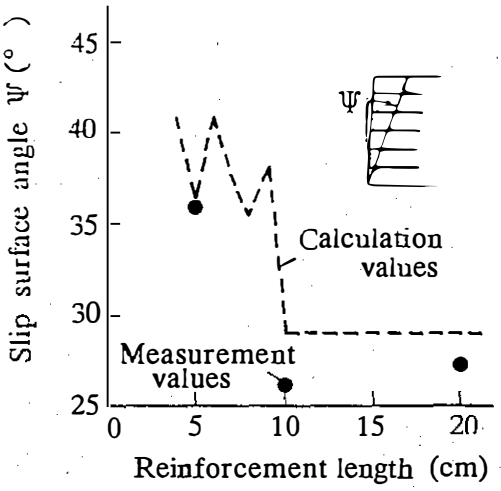

Figure 5 Effect of reinforcement length on Ψ

tion by defining the slip surface. For the purpose of defining the slip surface, implying a load on the embankment crest, 0.9cm-thick steel plates were placed, which were divided at a position 10cm from the top of the slope. The testing box was installed on a centrifuge model test device (Kitamoto et al., 1991), and the embankment was made to collapse through the repetition of a procedure in which the acceleration was increased by 10*G* (*G*: gravitational acceleration) at 5 minute intervals.

4 RESULTS AND DISCUSSION

4.1 Conditions at failure

The results for Case 2 are given in Figure 4 as an example of the observation results on the rupture positions in the reinforcements after the test. Stability analysis methods for slip surfaces of various shapes (e.g. compounded plane slip) have been proposed to date in the design of reinforced embankments. The shape of the slip surface in the case reported here could be approximated by a straight line. The slip line for the planar slip estimated from the stability calculations is shown together in the figure. Similar investigations were carried out for Cases 1 and 3. The slip surface angle Ψ determined from the deformation conditions photographed during the test in addition to the rupture positions of the reinforcements are compared with the calculated values in Figure 5. In the test result, the slip surface angle at reinforcement length = 5cm is larger than those at 10 and 20cm. This is because the slip surface occurring with small L passes outside the reinforced region in the upper parts of the embankment. The variation in Ψ recognised in the calculation results when L < 10cm is also caused by the passage of the slip surface outside the reinforced region. By reinforcing the slip surface with an adequate reinforcement length, one can transfer the slip surface inside the reinforced region and so reduce Ψ.

The calculation values for the equivalent embankment height H_{cp} in a 1*G* field worked out using the acceleration at the time of the collapse are compared with the measurement values in Figure 6. At L = 5cm, the embankment will collapse at H_{cp} half those in the cases where L = 10 and 20cm. Calculation results also show that H_{cp} increases with L, but after the L has reached a certain length the reinforcement effect remains constant while the reinforcement length increases. In Case 4, the embankment did not collapse even at the limit of the capacity of the test device (200*G*) (estimates for planar slip: Ψ = 39°, H_{cp} = 35m (235*G*)), indicating that dramatic improvements can be achieved in the stability of the reinforced embankment by turning an almost vertical slope into a slightly more gently sloping one at 1 : 0.5.

4.2 Transition of stability

In Figure 7, the calculation and measurement results for the 1*G* equivalent crest settlement ρ_p and the safety factor F_s against planar slip (the ratio between the sliding force of the slip soil

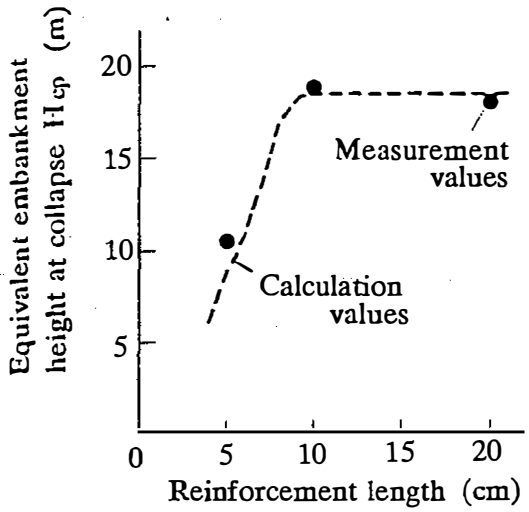

Figure 6 Effect of reinforcement length on Hcp

and the value obtained by adding the maximum shear resistance due to the reinforcements discussed in Section 2.2 to the shear resistance of the soil on the slip surface) are charted against the 1G equivalent embankment height H_P (the load placed on the embankment added as equivalent embankment height) for Cases 5 and 6, in which the slip surfaces were defined. As the acceleration increases, the sliding force of the slip soil increases and shear displacement results. At this point, pull-out occurs in the anchorage of the reinforcements traversing the slip surface and tensile force is generated with the elongation of the reinforcements. Furthermore, a direct shear condition results in the vicinity of the slip surface and the shear resistance due to the tensile force of the reinforcements increases and the shear displacement continues until a reinforcement effect required to balance the force of the slip soil is achieved. While settlement occurs as a result at the crest (see Figure 1), if the balance with the slip soil is not achieved even when the reinforcement effect is at its maximum, this will result in the collapse of the embankment. In this calculation method, these behaviours are treated as slippage of rigid bodies.

The calculation results show that as H_P increases, ρ_P increases and F_s decreases. In Case 5, ρ_P = 68.4mm immediately before collapse, or when F_s = 1 (H_P = 16.2m). The measurement results for the crest settlement on the slip surface agree closely with the calculation results. Quantitative evaluation of the stability of the reinforced embankment can, therefore, be made using the crest settlement, a value that can be measured, as well as from the safety factor. In Case 6, on the other hand, the rupture position of the reinforcements did not occur near the slip surface originally assumed, and $\Psi \cong 39°$. The investigations in Figure 7 are for $\Psi = 39°$. The calculation and measurement results

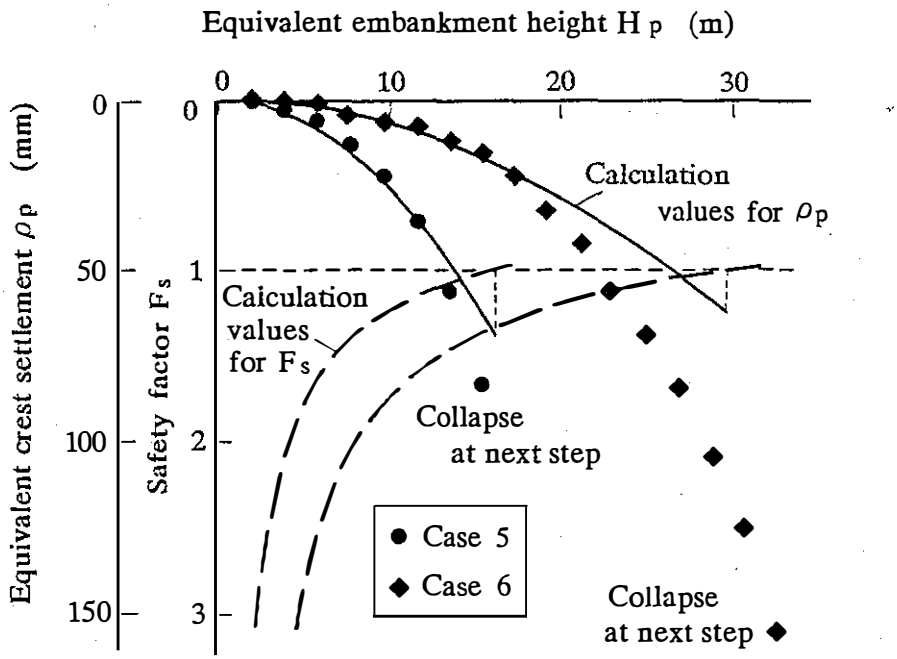

Figure 7 Changes in stability with deformation

agree closely while H_P is small, but the measurement results become larger than the calculation results as H_P increases because of the increase in the deformation around the slope sections due to such factors as bulging.

5 CONCLUDING COMMENTS

Centrifuge model tests were conducted to examine the validity of a stability analysis method taking deformation into account. The failure mode on steep reinforced embankments on hard ground was more or less planar and agreed closely with the results of calculations in which the crest settlement was used as the index for the stability of the embankment. The assumption of the direct shear conditions for the deformation of the embankment, however, means that there are limits to the application range of the analysis method when phenomena such as bulging occur in the slip soil itself.

REFERENCES

Abe, H. and Kitamoto, Y., 1989. Theoretical behavior of embedded geogrid under pull-out loading (in Japanese), *Proc. 4th Symp. on Geotextiles, ICIGS*, pp. 101–105.

Abe, H. and Kitamoto, T., 1990. Behavior and stability analysis of geogrid reinforced embankments (in Japanese), *Jour. JSSMFE*, vol. 30, No.3, pp. 185–196.

Jewell, R.A., Milligan, G.W.E., Sarsby, R.W. and Dubois, D., 1985. *Interaction between soil and geogrids, Polymer grid reinforcement*, Thomas Telford Ltd., London, pp.18–30.

Kitamoto, Y. and Abe, H., 1990. Stability evaluation of geogrid reinforced embankments on soft ground, *Proc. 9th ARCSMFE*, Bangkok, vol. 1, pp. 327–330.

Kitamoto. Y., Abe, H., Honda, M. and Jinki, R., 1991. Stability evaluation of reinforced embankments by centrifuge experiment (in Japanese), *Proc. 6th Symp. on Geotextiles, JCIGS*, pp. 63–67.